SYNERGISTIC USE OF SCATTEROMETER AND SCANSAR DATA FOR EXTRACTION OF SURFACE SOIL MOISTURE INFORMATION IN AUSTRALIA

Daniel Sabel, Zoltan Bartalis, Annett Bartsch, Marcela Doubkova, Stefan Hasenauer, Vahid Naeimi, Carsten Pathe, Wolfgang Wagner

Institute of Photogrammetry and Remote Sensing, Vienna University of Technology, Gusshausstrasse 27-29, 1040 Vienna, Austria

Abstract

The potential of the ERS-1/2 scatterometer global soil moisture product has been shown in several studies. The ASCAT sensor on-board the METOP satellite is extending the 16 year time series of the ERS-1/2 scatterometer as a source for extracting information for ocean and land applications. Calibrated ASCAT data will continue the scatterometer global soil moisture archive while improving both the spatial and temporal resolution.

A disaggregation scheme for spatial downscaling of the ASCAT soil moisture product, using a temporal stability analysis of medium resolution ScanSAR data from the ENVISAT ASAR sensor, has been developed. Furthermore, by transferring the change detection algorithm from the scatterometer to the ScanSAR data, also a 1 km Surface Soil Moisture product has been derived. The disaggregated scatterometer soil moisture product is evaluated in conjunction with the 1 km Surface Soil Moisture product in Australia. The influence of land cover on the performance of the products is considered.

Both high resolution products perform best in areas with less dense vegetation, such as agricultural lands and crop land. In areas with a dense vegetation canopy or deserts, the uncertainties in the extracted soil moisture values are large. The disaggregated product, while implicitly taking into account effects of land cover and surface roughness at different scales, provide a statistical approach to downscale regional soil moisture measurements to a finer spatial scale.

INTRODUCTION

Soil moisture is a key component in the global cycle of water and energy. In 2004, the Global Climate Observing System (GCOS) recognised soil moisture as an emerging Essential Climate Variable (GCOS, WMO et al. 2004). The development of soil moisture retrieval from passive and active microwave sensors has been ongoing since the 1970's. The Soil Moisture and Ocean Salinity (SMOS) mission, with launch expected in 2009, will provide soil moisture estimates from L-band radiometer with a resolution between 30 km and 50 km and a nominal repeat time of 3 days. (Barré, Duesmann et al. 2008). The ERS-1 and ERS-2 satellites have supplied scatterometer acquisitions since 1991 and with the launch in 2006 of the first satellite in the METOP series, METOP-A, the continuity of these measurements are ensured until 2021. The derivation of soil moisture estimates from scatterometers was initially applied to ERS-1/2 scatterometer data. The ERS-1/2 scatterometer soil moisture product has shown its potential to spatio-temporal soil moisture patterns on a global to continental scale in several studies (Ceballos, Scipal et al. 2005; Pellarin, Calvet et al. 2006; Fountaine, Louvet et al. 2007). The method has recently been transferred to the Advanced Scatterometer (ASCAT) flown onboard METOP-A. ASCAT provides a nearly daily global coverage with a resolution of 25 km and 50 km (Bartalis, Wagner et al. 2007). Dissemination of provisional ASCAT soil moisture products has been online since May 26 2008 via EUMETCAST. Furthermore, the soil moisture retrieval method has been transferred from the scatterometer domain to the SAR domain by using ENVISAT Advanced Synthetic Aperture Radar (ASAR) Global Monitoring (GM) mode data. The ASAR GM has a resolution of 1 km, which corresponds well to the resolution of many hydrologic models. The implementation of the ASAR soil moisture product for Australia was carried out within the project "SHARE extension", which is part of the European Space Agency's TIGER Initiative. The third and final soil moisture product evaluated in this paper was generated using a downscaling scheme that has been developed

within the framework of EUMETSAT's Satellite Application Facility in support of Hydrology and Water Management (H-SAF) (Hasenauer, Wagner et al. 2006). By applying the downscaling method to 50 km ASCAT soil moisture measurements, a 1 km disaggregated product has been generated. This paper briefly explains the three methods used to derive the soil moisture datasets and presents a spatial and a temporal intercomparison as well as a spatial comparison with rainfall data based on in-situ measurements.

METHOD

Data sets and algorithms

Both scatterometer and SAR data were used in the study. Scatterometer data from the METOP-A ASCAT have a resolution of 50 km. With a nearly daily revisit time, this data is well suitable for change detection. The data used in this study were commissioning phase data and thus might not correspond to the final calibration. However, a recent comparison with ERS-2 scatterometer data proved good agreement (Naeimi, Bartalis et al. 2008 (early online release, posted January 2008)). The algorithm to derive soil moisture from ASCAT is the same as has been previously applied to the ERS-1 and ERS-2 Active Microwave Instrument (AMI) scatterometers. Each pixel on the ground is observed nearly simultaneously with three acquisitions by the scattometer's for, mid and aft beams. The three acquisitions are used for incidence angle dependency correction by normalising the backscatter measurements to 40 degrees incidence angle and subsequently for vegetation correction. In a second step, backscatter references for dry and wet soil surface conditions are derived. In the final step, each backscatter measurements is scaled linearly between the dry and wet reference to get a relative measure of the water saturation of the top layer of the soil (Wagner, Lemoine et al. 1999). Due to the short time series of ASCAT data (in this study March to December 2007), the wet and dry references were derived from the ERS-1/2 scatterometer data. The 50 km ASCAT soil moisture product is here denoted "ASCAT SM". The soil moisture estimates were resampled with the Hamming method to a grid with 12.5 km spacing.

The SAR data were provided by ENVISAT's ASAR sensor. The ASAR sensor is operated in C-band at 5.331 GHz. In GM mode, data is acquired with a resolution of 1 km and a radiometric resolution of about 1.2 dB. The ASAR sensor allows a wide swath of 405 km by means of the ScanSAR technique, which in combination with a 100% potential duty cycle results in a greatly improved coverage compared to the other SAR modes with higher spatial resolutions. For Australia in general more than 350 acquisitions are available at each location for the period December 2004 – June 2008. In an initial step, all ScanSAR backscatter and local incidence angle images are resampled to a global grid and stored in a database. Secondly, the local incidence angle dependency of the backscatter measurements is normalised by fitting the full time series of data at each location and then reverting each measurement to a reference angle of 30 degrees. In a third step, backscatter references for wet and dry soil moisture conditions are derived from the time series data for each location. The derivation of the dry and wet reference uses probabilities of dry and wet soil surface conditions derived from the long time series of ERS-1/2 scatterometer data. Due to the low probability of acquiring a backscatter measurement for saturated soil moisture conditions in generally dry areas, a pragmatic correction of the wet reference was implemented in which the reference is increased to a maximum of -6 dB with the constraint that the difference between the wet reference at the 30 degrees reference incidence angle ($\sigma^0_{wet}(30)$) and the corresponding dry reference ($\sigma^0_{dry}(30)$) must not exceed 10 dB. Finally, all backscatter measurements ($\sigma^0(30,t)$) are scaled between the location specific dry and wet reference according to equation (1) .

$$m_s(t) = \frac{\sigma^0(30,t) - \sigma^0_{dry}(30)}{\sigma^0_{wet}(30) - \sigma^0_{dry}(30)} \quad (1)$$

The output is the 1 km ASAR Surface Soil Moisture product, here denoted "ASAR SM", which corresponds to the same parameter as in the ASCAT SM, i.e., a relative measure of the water saturation of the top layer of the soil.

The third soil moisture product analysed in this paper is based on a downscaling method which was applied to the 50 km ASCAT SM. The method is based on the concept of temporal stability introduced by (Vachaud, Passerat de Silans et al. 1985) and applied to soil moisture fields and radar backscatter (Wagner, Pathe et al. 2008). In the following equations, the subscript *l* stands for the local (1 km) scale and the subscript *r* stands for regional (50 km) scale. A linear relationship is assumed between the local scale and regional scale soil moisture (θ) according to equation (2).

$$\theta_l(x,y,t) = c_{lr}(x,y) + d_{lr}(x,y)\theta_r(t) \tag{2}$$

The parameters c_{lr} and d_{lr} account for the bias and the dynamics between the soil moisture on the two scales and are derived for each location according to

$$c_{lr}(x,y) = \frac{a(x,y,t) + b(x,y,t)\sigma^0_{dry,r}(t) - \sigma^0_{dry,l}(x,y,t)}{S_l(x,y,t)} \tag{3}$$

$$d_{lr}(x,y) = b(x,y,t)\frac{S_r(t)}{S_l(x,y,t)} \tag{4}$$

where $\sigma^0_{dry,r}$ and $\sigma^0_{dry,l}$ correspond to the backscatter references for completely dry soil conditions on the two scales. S_r and S_l represent the sensitivities to soil moisture, i.e., the difference between the backscatter references for dry and wet soil conditions. The parameters *a* and *b* describes the bias and the dynamics between the radar backscatter on the two scales according to

$$\sigma^0_l(x,y,t) = a(x,y,t) + b(x,y,t)\sigma^0_r(t) \tag{5}$$

The parameters *a* and *b* were derived for each location using linear regression on the time series of ASAR backscatter acquisitions, with the regional backscatter measurements ($\sigma^0_r(t)$) being formed by spatial averaging of the local measurements ($\sigma^0_l(t)$). The 1 km disaggregated soil moisture product is here denoted “ASCAT DSM”.

For the land cover analysis the USGS Global Land Cover Classification (GLCC) version 2.0 was used. The dataset has a resolution of 1 km and has 23 classes. A reclassification was carried out in accordance with the USGS Land Use/Land Cover System (LULC) (Modified Level 2) in order to obtain four representative classes here denoted “Cropland”, “Rangeland”, “Forest” and “Barren or Sparsely Vegetated”. The reclassified Cropland class is dominated (>99%) by Dryland Cropland and Pasture but also includes locations with irrigated cropland and pasture and cropland mixed with patches of grassland or woodland. Rangeland include grassland, shrubland and savanna. The Forest class includes all types of forest, in this study dominated (>99%) by Evergreen Broadleaf Forest. The class “Barren or Sparsely Vegetated” does not have a parent class in the LULC System and thus did not require reclassification.

For a spatial comparison with rainfall patterns, the Monitoring Product of the Global Precipitation Climatology Centre (GPCC) was used (Schneider, Fuchs et al. 2008). The product represents total monthly rainfall and is interpolated to 1.0° spatial resolution from an extensive network of in-situ stations.

Study area

The study was made over south eastern Australia, including the Murray Darling Basin. This region has had more than a decade of low rainfall and major research effort has been directed to better understand the recent climate and its variability (Murphy and Timbal 2008). The Darling is a tributary of the Murray. Both rivers have their source in the Great Dividing Range which is characterised by humid subtropical climate. The lower western parts of the basin on the contrary feature dry subtropical climate and semi deserts. Precipitation varies considerably from year to year over the central areas. River regulation by dams is also altering inundation patterns of wetlands (Frazier and Page 2006). The

adjacent basins in central Australia are characterised by a number of floodplains and playas which refill only during high inflow events. A prominent example is the Cooper creek floodplain (Capon 2007) which connects to the Yamma Yamma playa.

RESULTS

Spatial patterns

Figure 1 shows soil moisture conditions around noon on 26 June 2007. From left to right the ASCAT SM, ASAR SM and ASCAT DSM are shown. Note that in all the spatial images of ASAR SM, grey pixels correspond to locations that have been masked out due to expected high uncertainties in the soil moisture estimates. Figure 2 shows the monthly mean conditions of ASCAT SM, ASAR SM and GPCC monthly rainfall for March 2007. Figure 4 shows the monthly mean conditions for June 2007. The patchy soil moisture patterns northwest of the Murray Darling Basin in Figure 2 and Figure 4 are the results of, respectively, heavy rainfall in January (Figure 3) and May (Figure 5).

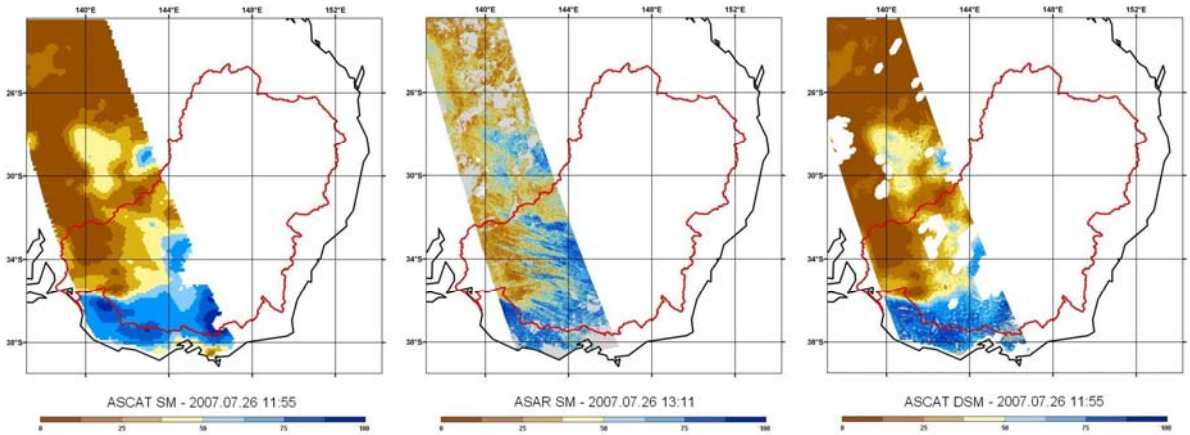

Figure 1: **From left to right; ASCAT SM, ASAR SM and ASCAT DSM on 26 July 2007. The time difference between the ASCAT and the ASAR acquisition is 1 hour 16 minutes.**

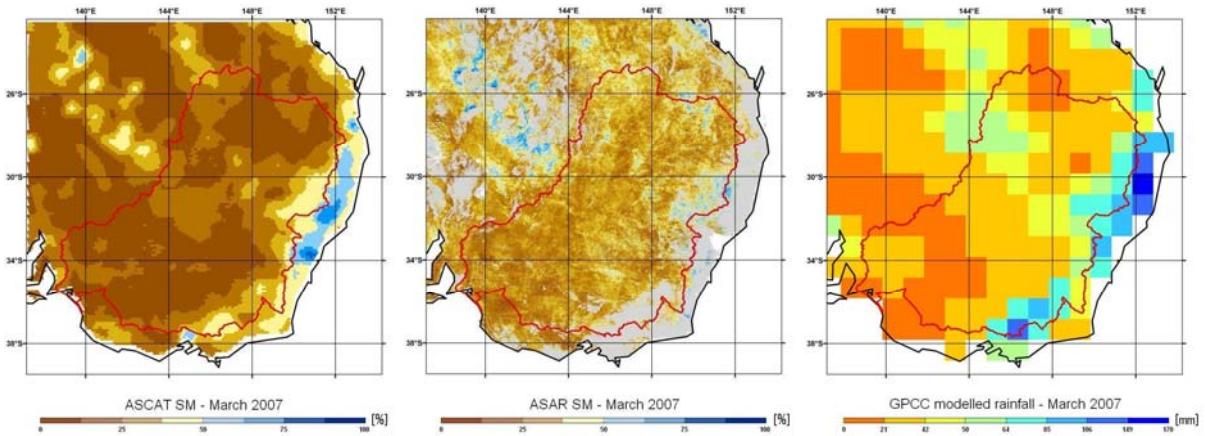

Figure 2**: Monthly mean soil moisture for March 2007 based on the ASCAT SM and ASAR SM products. The rightmost graphic is total rainfall (GPCC) for the same month. Grey pixels in the ASAR SM image have been masked out due to expected high uncertainties.**

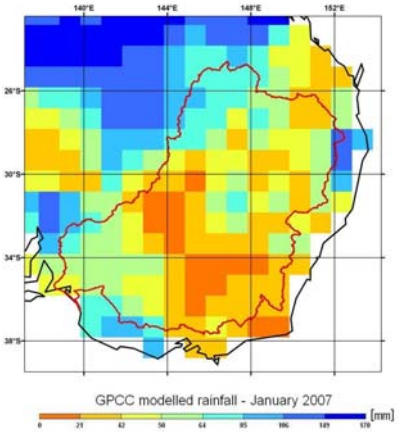

Figure 3: **Monthly total rainfall for January 2007. High amounts can be seen north and northwest of the Murray Darling Basin.**

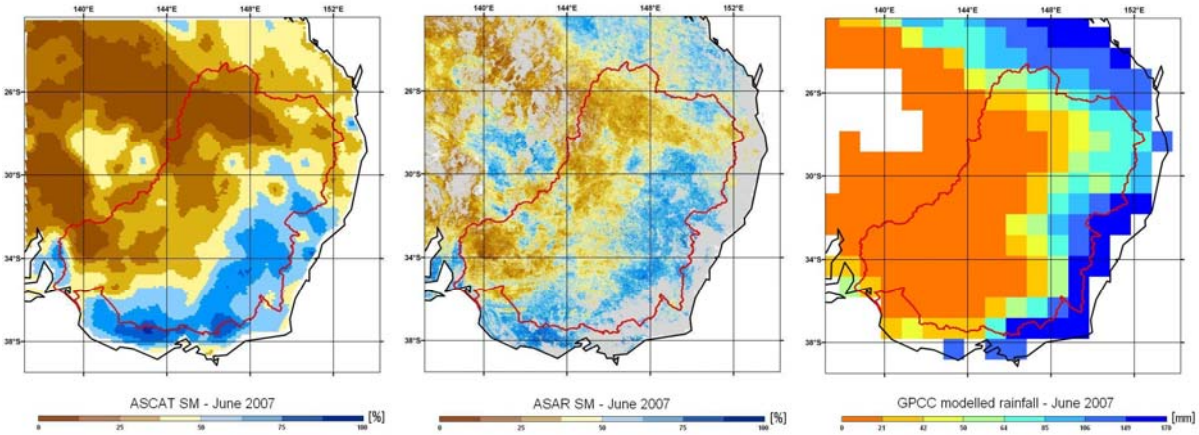

Figure 4: **Monthly mean soil moisture for June 2007. The rainfall in the rightmost graph shows high values along the eastern coast. Note the spatial correlation between the two soil moisture images.**

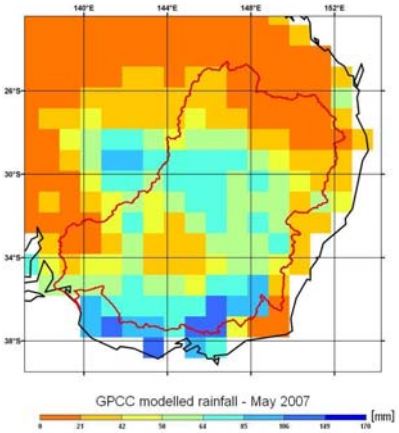

Figure 5: **Monthly rainfall for May 2007.**

Temporal correlation

Time series data from ASCAT SM, ASAR SM and ASCAT DSM were extracted at evenly distributed locations over the test area with a sampling distance of 12.5 km. For each location, the time series' for the three datasets were reduced to nearly simultaneous acquisitions, allowing a time difference of 2 hours. Only time series data for which at least 30 nearly simultaneous acquisitions could be identified were included. Furthermore, only locations in areas of homogeneous land cover were included. Homogeneous land cover were defined as a minimum Hamming weighted coverage of 75% for a single land cover type over a 40 km footprint. Finally, the ASAR SM was compared to the

ASCAT SM and ASCAT DSM for the remaining 2173 locations. The Pearson correlation coefficient (R), root mean square error (RMSE) and bias was calculated at each location. The results of the comparison between ASAR SM and ASCAT SM and are shown in Figure 6. The statistics for Barren or Sparsely Vegetated land is not displayed in the box plot graphics because no locations with homogeneous land cover for that category could be identified. Including also areas with heterogeneous land cover, five locations could be identified with enough measurements. For those five locations the mean statistics for the Barren or Sparsely Vegetated category were as follows: R: 0.08, RMSE: 32.9%, bias: 26.9%.

To account for the noise of the ASAR GM measurements and the difference in spatial resolution between the ASAR and the ASCAT measurements, a Hamming resampling of the ASAR SM data to 40 km resolution was carried out. The comparison of ASCAT SM and ASAR SM was then re-iterated using the resampled ASAR SM values. The results are presented in Figure 7. Comparing to Figure 6 it can be seen that the correlation increased significantly while the RMSE decreased. The bias remained significantly above zero.

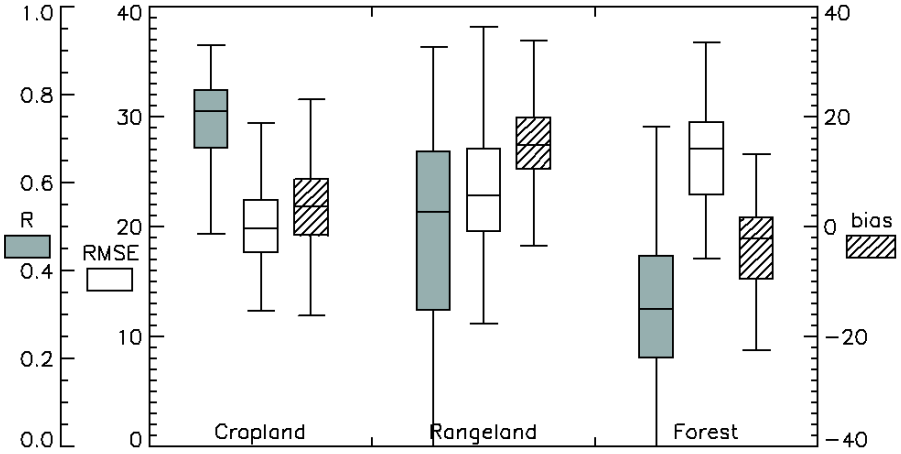

Figure 6: **Comparison between the 1 km ASAR SM and the 50 km ASCAT SM for the test area. The bias shows how much higher the ASAR SM generally is compared to the ASCAT SM.**

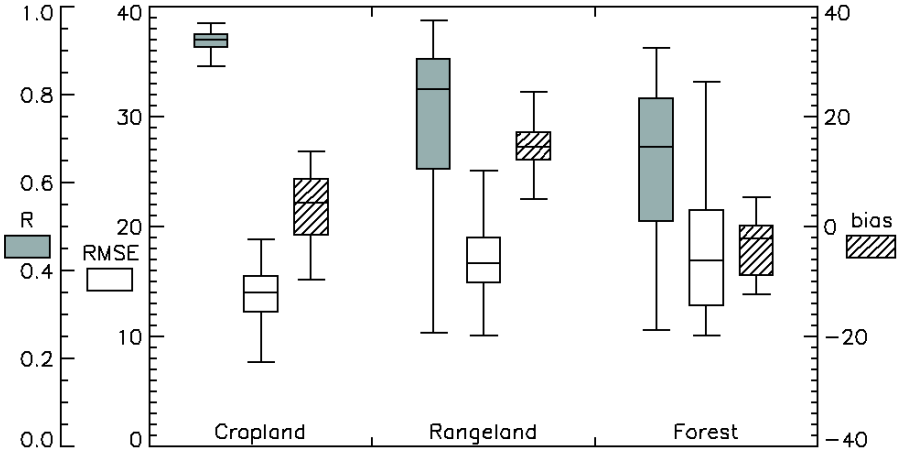

Figure 7: **Comparison between Hamming resampled ASAR SM and 50 km ASCAT SM. Comparing to Figure 6 it can be seen that the correlation increased significantly while the RMSE decreased. The bias remained significantly above zero.**

The comparison between ASCAT DSM and ASAR SM showed very small differences in the statistics compared to the ASCAT SM versus ASAR SM analysis shown in Figure 6. A summary of the mean values of the statistics from the temporal analysis is shown in Table 1. Comparing the values of columns 2 and 4 in Table 1, it can be seen that the bias in general was slightly corrected, while the RMSE was slightly increased during the disaggregation.

	ASAR SM – ASCAT SM				Haming resampled ASAR SM – ASCAT SM				ASAR SM – ASCAT DSM			
	a	**b**	**c**	**d***	**a**	**b**	**c**	**d***	**a**	**b**	**c**	**d***
Mean R	0.73	0.48	0.32	0.08*	0.91	0.74	0.65	0.53*	0.73	0.48	0.31	0.13*
Mean RMSE [%]	20.2	23.8	26.8	32.9*	13.9	17.3	17.3	24.8*	20.6	23.8	27.9	29.7*
Mean bias [%]	3.5	15.2	-3.7	26.9*	3.3	14.8	-3.6	23.3*	2.7	15.0	-1.2	20.7*

Table 1: **Mean values of the statistics from the temporal analysis for the four land cover categories; a) Cropland, b) Rangeland, c) Forest and d) Barren or Sparsely Vegetated. *Note that due to limited coverage for the Barren or Sparsely Vegetated category in the test area, it was necessary to include locations with non-homogeneous land cover when calculating the statistics for that land cover category.**

DISCUSSION

The ASAR GM data differs from the ASCAT data in most aspects. Apart from the spatial resolution, the radiometric resolution is much lower in the ASAR data with an estimated 1.2 dB which is more than twice the noise of ASCAT. With a typical sensitivity to soil moisture between 5 dB and 10 dB over the study area, only a few classes are expected to be distinguishable in the ASAR SM product. Furthermore, the algorithm for extracting soil moisture from the ASAR data is a simplification of the scatterometer algorithm, e.g., there is no explicit vegetation correction. Despite these facts, Figure 1, Figure 2 and Figure 4 demonstrate the spatial agreement between the ASCAT SM and the ASAR SM products. The ASAR SM displays interesting fine scale patterns not visible in the ASCAT SM. Figure 2 and Figure 4 show the monthly mean conditions of ASCAT SM, ASAR SM and GPCC monthly rainfall for, respectively, March and June 2007. Overall spatial soil moisture patterns correlate with the distribution of rainfall. However, the patchy soil moisture patterns northwest of the Murray Darling Basin do not correlate. The explanation is that the area is semi-arid but can become and remain flooded from heavy rainfall. Runoff from the surrounding mountainous areas also adds to the distribution of water over the surface. The result is a time lag between rainfall and soil moisture. The patchy soil moisture conditions in March and June correlate well with rainfall in January (Figure 3) and May (Figure 5), respectively.

The temporal correlation analysis quantifies the agreement between the ASAR SM and ASCAT SM, summarised in Table 1. From Figure 6 and Figure 7 it is clear that there is a systematic bias in the ASAR SM to give higher estimates than the ASCAT SM. This could be explained by an underestimation of the backscatter reference for saturated soil conditions resulting from the low probability of acquiring backscatter measurements representative of completely wet soils from the relatively short times series (3.5 years) of ASAR GM data, especially over dry areas. The best results were achieved for the Cropland and Rangeland categories. The low correlation for forests could be explained by the low backscatter response to the ground surface due to the vegetation canopy layer. In the case of Barren or Sparsely vegetated land, volume scattering in sandy soils together with high response from stones which act as corner reflectors can make the backscatter characteristics erratic, resulting in unreliable soil moisture estimates. When resampling the ASAR SM to 40 km resolution using the Hamming method, the radiometric noise is greatly reduced while the spatial scale is matched with that of the ASCAT measurements. The results in Figure 7 and column 3 in Table 1 show a significant improvement in correlation and RMSE, demonstrating the prominent influence of the noise in the ASAR backscatter acquisitions on the ASAR SM. The RMSE remained above 13% for all land cover categories, partially as a result of the systematic bias.

The spatial image of the ASCAT DSM in Figure 1 shows that spatial details are added during the downscaling. Comparing columns 2 and 4 in Table 1, it can be seen that the disaggregation only slightly changed the statistics when compared to ASAR SM. However, due to the nature of the disaggregation method, which is a linear operation with spatially dependent coefficients, it is expected that the overall *spatial* correlation is improved. Therefore, a spatial analysis, preferably with ground reference data, would be of interest.

CONCLUSION

The spatial patterns in the ASCAT SM and ASAR SM products corresponded well with rainfall. The 1 km ASAR SM product showed interesting spatial details not visible in the 50 km ASCAT SM. The temporal correlation between the ASAR SM and ASCAT SM was strong, considering the difference in

scale and high noise of the ASAR GM data, with best results for the Cropland category with R=0.73. When comparing ASCAT SM to Hamming resampled ASAR SM, RMSE values decreased and correlations increased significantly with R=0.91 for Cropland. These results illustrate the prominent influence of the high noise in the ASAR GM backscatter measurements. There was a bias in the ASAR SM to give higher estimates than the ASCAT SM. This can be explained by an underestimation of the backscatter reference for wet surface soil conditions resulting from the low probability of catching backscatter measurements for completely wet soils from the relatively short times series (3.5 years) of ASAR GM data. Further development in the derivation of the wet reference is required.

Further analysis, including uncertainty estimates, are required to assess the value of the disaggregated product. An analysis based on comparing sets of soil moisture fields, rather than the temporal analysis carried out in this paper, would be beneficial for evaluating the disaggregated product. The 1 km disaggregated ASCAT product is still in a development phase.

A comparison of the datasets to ground reference data is required in order to evaluate the spatial details shown in the ASAR SM and to quantify the added value of the disaggregation method applied to ASCAT SM data.

REFERENCES

Barré, H. M. J. P., Duesmann, B. and Kerr, Y. H. (2008). "SMOS: The Mission and the System." IEEE Transactions on Geoscience and Remote Sensing **46**(3):pp 587-593.

Bartalis, Z., Wagner, W., Naeimi, V., Hasenauer, S., Scipal, K., Bonekamp, H., Figa, J. and Anderson, C. (2007). "Initial soil moisture retrievals from the METOP-A Advanced Scatterometer (ASCAT)." Geophysical Research Letters **34**(L20401).

Capon, S. J. (2007). "Effects of flooding on seedling emergence from the soil seed bank of a large desert floodplain." Wetlands **27**:pp 904-914.

Ceballos, A., Scipal, K., Wagner, W. and Martínez-Fernández, J. (2005). "Validation of ERS scatterometer-derived soil moisture data in the central part of the Duero Basin, Spain." Hydrological Processes **19**(8):pp 1549-1566.

Fountaine, B., Louvet, S. and Roucou, P. (2007). "Fluctuations in annual cycles and inter-seasonal memory in West Africa: rainfall, soil moisture and heat fluxes." Theoretical and Applied Climatology **88**(1-2):pp 57-70(14).

Frazier, P. and Page, K. (2006). "The effect of river regulation on floodplain wetland inundation, Murrumbidgee River, Australia." Marine and Freshwater Research **57**(2):pp 133-141.

GCOS, WMO, UNESCO, I. o., UNEP and ICSU (2004). Implementation Plan for the Global Observing System for Climate in Support of the UNFCCC.

Hasenauer, S., Wagner, W., Scipal, K., Naeimi, V. and Bartalis, Z. (2006). Implementation of Near Real-Time Soil Moisture Product in the SAF Network Based on METOP ASCAT Data. 2006 EUMETSAT Meteorological Satellite Conference, Helsinki, Finland.

Naeimi, V., Bartalis, Z. and Wagner, W. (2008 (early online release, posted January 2008)). "ASCAT Soil Moisture: An Assessment of the Data Quality and Consistency with the ERS Scatterometer Heritage." Journal Of Hydrometeorology.

Pellarin, T., Calvet, J.-C. and Wagner, W. (2006). "Evaluation of ERS scatterometer soil moisture products over a half-degree region in southwestern France." Geophysical Research Letters **33**(L17401).

Schneider, U., Fuchs, T., Meyer-Christoffer, A. and Rudolf, B. (2008). Global Precipitation Analysis Products of the GPCC, Global Precipitation Climatology Centre (GPCC), Deutsche Wetterdienst.

Vachaud, G., Passerat de Silans, A., Balabanis, P. and Vauclin, M. (1985). "Temporal Stability of Spatially Measured Soil Water Probability Density Function." Soil Science Society of America **49**:pp 822-828.

Wagner, W., Lemoine, G. and Rott, H. (1999). "A Method for Estimating Soil Moisture from ERS Scatterometer and Soil Data." Remote Sensing of Environment **70**(2):pp 191-207.

Wagner, W., Pathe, C., Doubkova, M., Sabel, D., Bartsch, A., Hasenauer, S., Blöschl, G., Scipal, K., Martínez-Fernández, J. and Löw, A. (2008). "Temporal Stability of Soil Moisture and Radar Backscatter Observed by the Advanced Synthetic Aperture Radar (ASAR)." Sensors **8**:pp 1174-1197.